

## Supporting Information

### Solid-state NMR analysis reveals a possible calcium binding site of pradimicin A

Takashi Doi,<sup>a</sup> Yu Nakagawa,<sup>b</sup> K. Takegoshi;<sup>a,\*</sup>

<sup>a</sup>Department of Chemistry, Graduate School of Science, Kyoto University, Kitashirakawa Oiwake-cho, Sakyo-ku,  
Kyoto 606-8502, Japan

<sup>b</sup>Department of Applied Molecular Biosciences, Graduate School of Bioagricultural Sciences, Nagoya University,  
Furo-cho, Chikusa-ku, Nagoya 464-8601, Japan

Corresponding Author

\*takeyan@kuchem.kyoto-u.ac.jp

## Contents

1. General remarks
2. Preparation of the complex of [18- $^{13}\text{C}$ ]PRM-A with  $^{111}\text{Cd}^{2+}$  and Man-OMe
3. Preparation of the complex of [ $^{13}\text{C}_{12}$ ]PRM-A with  $^{111}\text{Cd}^{2+}$  and Man-OMe
4. General solid-state NMR experimental parameters
5. Solid-state  $^{111}\text{Cd}$  1D cross polarization (CP)/magic angle spinning (MAS) NMR experiment
6. Solid-state  $^{13}\text{C}$ - $^{111}\text{Cd}$  REDOR NMR experiment
7. Solid-state  $^{111}\text{Cd}$  1D CP/MAS NMR experiment with a Gaussian  $\pi$  pulse
8. Solid-state  $^{13}\text{C}$ - $^{111}\text{Cd}$  frequency selective REDOR (FSR) NMR experiment
9. References for Supporting Information

## 1. General remarks

PRM-A was isolated from the fermentation broth of *Actinomyces sp.* TP-A0019. [2-<sup>13</sup>C]AcONa (>99 atom % <sup>13</sup>C) and [1-<sup>13</sup>C]alanine (>99 atom % <sup>13</sup>C) were purchased from Taiyo Nippon Sanso Corporation (Tokyo, Japan). <sup>111</sup>CdCl<sub>2</sub> (95.5 atom % <sup>111</sup>Cd) was purchased from Trace Sciences International. All other chemicals and reagents were purchased from chemical companies and used without further purification.

## 2. Preparation of the complex of [18-<sup>13</sup>C]PRM-A with <sup>111</sup>Cd<sup>2+</sup> and Man-OMe

To a solution of [18-<sup>13</sup>C]PRM-A (15.2 mg, 15.9 μmol) in distilled water (1.5 mL) was added 200 mM <sup>111</sup>CdCl<sub>2</sub> (159 μL, 31.8 μmol, 2 equiv.) and 100 mM Man-OMe (3.98 mL, 397.5 μmol, 25 equiv.) at room temperature. The pH of the solution was adjusted to 4.2 with 1N NaOH. The resulting mixture was incubated at 60°C for 30 min and room temperature for 15 h. After centrifugation at 10,000 g for 10 min, the supernatant was removed by decantation and the precipitate was washed two times with distilled water. After centrifugation at 10,000 g for 5 min, and then dried in vacuo for 1 h to afford the solid aggregate composed of the ternary complex of [18-<sup>13</sup>C]PRM-A with <sup>111</sup>Cd<sup>2+</sup> and Man-OMe (15.0 mg) as a red powder.

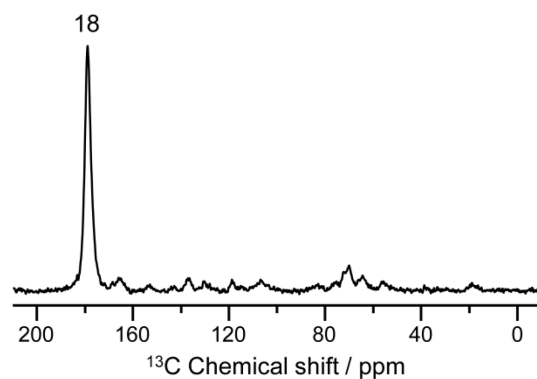


Figure S1.  $^{13}\text{C}$  1D spectrum of the complex of  $[18\text{-}^{13}\text{C}]\text{PRM-A}$ .  $\delta = 179$  ppm signal is of the C18 carbon of PRM-A.

Relatively small peaks are derived from natural abundant  $^{13}\text{C}$  of PRM-A and Man-OMe.

### 3. Preparation of the complex of [ $^{13}\text{C}_{12}$ ]PRM-A with $^{111}\text{Cd}^{2+}$ and Man-OMe

To a solution of [ $^{13}\text{C}_{12}$ ]PRM-A (13.3 mg, 13.9  $\mu\text{mol}$ ) in distilled water (1.5 mL) was added 200 mM  $^{111}\text{CdCl}_2$  (139  $\mu\text{L}$ , 27.8  $\mu\text{mol}$ , 2 equiv.) and 100 mM Man-OMe (3.48 mL, 347.5  $\mu\text{mol}$ , 25 equiv.) at room temperature. The pH of the solution was adjusted to 4.2 with 1N NaOH. The resulting mixture was incubated at 60°C for 30 min and room temperature for 15 h. After centrifugation at 10,000  $g$  for 10 min, the supernatant was removed by decantation and the precipitate was washed two times with distilled water. After centrifugation at 10,000  $g$  for 5 min, and then dried in vacuo for 1 h to afford the solid aggregate composed of the complex of [ $^{13}\text{C}_{12}$ ]PRM-A with  $^{111}\text{Cd}^{2+}$  and Man-OMe (11.4 mg) as a red powder.

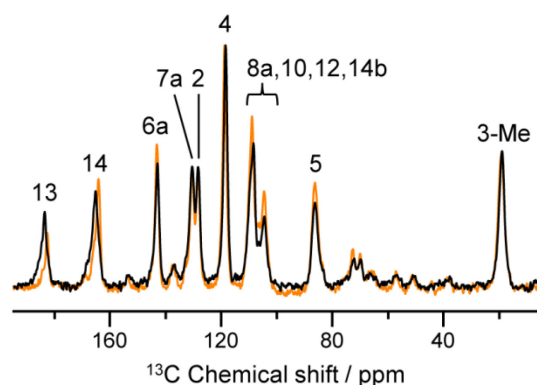


Figure S2.  $^{13}\text{C}$  1D spectra of the complex of  $[^{13}\text{C}_{12}]\text{PRM-A}$  with  $^{111}\text{Cd}^{2+}$  (black), and the complex of  $[^{13}\text{C}_{12}]\text{PRM-A}$  with  $\text{Ca}^{2+}$  (orange).<sup>1</sup> We assign the signals to the  $^{13}\text{C}$ -enriched positions as we assigned previously.<sup>1</sup>  $^{13}\text{C}_{13}/^{13}\text{C}_{14}$  chemical shifts of the complex of  $[^{13}\text{C}_{12}]\text{PRM-A}$  with  $^{111}\text{Cd}^{2+}$  are  $\delta = 184.0$  ppm (C13) and  $\delta = 165.4$  ppm (C14), respectively. Those of the complex of  $[^{13}\text{C}_{12}]\text{PRM-A}$  with  $\text{Ca}^{2+}$  are  $\delta = 182.9$  ppm (C13) and  $\delta = 164.5$  ppm (C14), respectively. The chemical shift differences between other respective  $^{13}\text{C}$  peaks are within  $\pm 0.3$  ppm (see Table S1). The peak shifts of C13/C14 are considered to originate in the change of the coordinated metal ion. These shifts are consistent that both the  $\text{Ca}^{2+}$  and  $\text{Cd}^{2+}$  binding sites are the C13/C14 site of the anthraquinone moiety of PRM-A.

Table S1.  $^{13}\text{C}$  chemical shifts (ppm) of the complex of  $[^{13}\text{C}_{12}]\text{PRM-A}$  with  $^{111}\text{Cd}^{2+}$  and that with  $\text{Ca}^{2+}$  (the  $^{13}\text{C}$  1D spectra are shown in figure S2). The differences of the respective chemical shifts are also shown in the fourth column.

	the complex of $[^{13}\text{C}_{12}]\text{PRM-A}$ with $^{111}\text{Cd}^{2+}$	the complex of $[^{13}\text{C}_{12}]\text{PRM-A}$ with $\text{Ca}^{2+}$	difference
C13	184.0	182.9	1.1
C14	165.4	164.5	0.9
C6a	143.2	143.3	-0.1
C7a	130.6	130.6	0.0
C2	128.4	128.5	-0.1
C4	118.5	118.8	-0.3
C8a,10,12,14b (1)	108.6	108.9	-0.3
C8a,10,12,14b (2)	104.4	104.6	-0.2
C5	86.3	86.2	0.1
C3-Me	18.6	18.6	0.0

#### 4. General solid-state NMR experimental parameters

Through all solid-state NMR experiments, we used the following canon parameters:  $^1\text{H}$  CP amplitude = 70 kHz,  $^1\text{H}$  decoupling power = 100 kHz, and the pulse delay = 1.2 s. The  $^{13}\text{C}$  chemical shifts were calibrated in ppm relative to TMS by taking the  $^{13}\text{C}$  chemical shift for the methine carbon nucleus of solid adamantane (29.5 ppm) as an external reference standard. The  $^{111}\text{Cd}$  chemical shifts were calibrated in ppm relative to solid  $\text{Cd}(\text{ClO}_4)_2 \cdot 6\text{H}_2\text{O}$  as an external reference standard.

#### 5. Solid-state $^{111}\text{Cd}$ 1D cross polarization (CP)/magic angle spinning (MAS) NMR experiment

$^{111}\text{Cd}$  1D CP/MAS experiment was carried out at a MAS frequency of 18 kHz at room temperature. The Hahn echo, ramped-amplitude CP (RAMP-CP) and two pulse phase-modulated (TPPM) decoupling were used with the CP contact time = 2.5 ms, the Hahn echo interval = 55.556  $\mu\text{s}$ , the  $^{111}\text{Cd}$   $\pi$  pulse length = 11  $\mu\text{s}$  (45 kHz), the dwell time = 5  $\mu\text{s}$ , the acquisition length = 1024, and the number of accumulation = 10000. Free induction delay (FID) was cut to 512 points and zero-filled up to 4096 points. An exponential window function of 80 Hz was applied prior to FT.

#### 6. Solid-state $^{13}\text{C}$ - $^{111}\text{Cd}$ REDOR NMR experiment

For the  $^{13}\text{C}$ - $^{111}\text{Cd}$  REDOR experiment, the conventional REDOR sequence with a single recoupling pulse on the  $^{13}\text{C}$  spins and all rotor-synchronized  $\pi$  pulses with the XY-8 phase cycles applied on-resonance to the center of the two  $^{111}\text{Cd}$  signals was used. All of the experiments were carried out at a MAS frequency of 12.5 kHz at room temperature.



RAMP-CP and TPPM decoupling were used. Pulse sequence parameters were the CP contact time = 4.0 ms (the complex of [ $^{13}\text{C}_{12}$ ]PRM-A) and 1 ms (the complex of [ $18\text{-}^{13}\text{C}$ ]PRM-A), the  $^{13}\text{C}$   $\pi$  pulse length = 15  $\mu\text{s}$  (33 kHz), the  $^{111}\text{Cd}$   $\pi$  pulse length = 15  $\mu\text{s}$  (33 kHz), the dwell time = 20  $\mu\text{s}$ , the acquisition length = 1024, and the number of accumulation = 2048 (the complex of [ $^{13}\text{C}_{12}$ ]PRM-A) or 4096 (the complex of [ $18\text{-}^{13}\text{C}$ ]PRM-A). FIDs were zero-filled up to 4096 points. An exponential window function of 20 Hz was applied. The  $^{13}\text{C}$  signal intensities obtained by the REDOR experiments ( $S_R$ ) were scaled by those obtained by the respective REDOR reference experiments ( $S_0$ ), which include no  $\pi$  pulses on the  $^{111}\text{Cd}$  channel. The REDOR dephasing curves are calculated numerically with the equations found in reference 2 and 3.

#### 7. Solid-state $^{111}\text{Cd}$ 1D CP/MAS NMR experiment with a Gaussian $\pi$ pulse

The efficiency of the Gaussian  $\pi$  pulses were confirmed using the pulse sequence shown in figure S5a and S5b with a MAS frequency of 12.5 kHz at room temperature. RAMP-CP and TPPM decoupling were used. Pulse sequence parameters were same as the  $^{111}\text{Cd}$  normal Hahn echo experiment, except for, the  $^{111}\text{Cd}$   $\pi/2$  pulse length = 4.1  $\mu\text{s}$  (61 kHz), the z-filter length = 5.12 ms (figure S5c-1, c-2) or 5.44 ms (figure S5c-3), the Hahn echo interval = 80  $\mu\text{s}$ , the  $^{111}\text{Cd}$  hard  $\pi$  pulse length = 15  $\mu\text{s}$  (33 kHz), the  $^{111}\text{Cd}$  Gaussian  $\pi$  pulse length = 640  $\mu\text{s}$  (maximum RF strength of 1.5 kHz), the increment of Gaussian pulse steps = 128, the acquisition length = 2048, and the number of accumulation = 2048.

## 8. Solid-state $^{13}\text{C}$ - $^{111}\text{Cd}$ frequency selective REDOR (FSR) NMR experiment

For the  $^{13}\text{C}$ - $^{111}\text{Cd}$  FSR experiment, a single recoupling hard  $\pi$  pulse was applied on the  $^{13}\text{C}$  spins; all rotor-synchronized hard  $\pi$  pulses with the XY-8 phase cycles are applied similar to REDOR on the  $^{111}\text{Cd}$  spins; and a Gaussian selective  $\pi$  pulse are applied on-resonance to one of the  $^{111}\text{Cd}$  signals. By these arrangements, we can recouple all of the  $^{13}\text{C}$  spins with the selected  $^{111}\text{Cd}$  spin. All of the experiments were carried out at a MAS frequency of 12.5 kHz at room temperature. Experimental parameters were the same as the REDOR experiments and the  $^{111}\text{Cd}$  Gaussian  $\pi$  pulse experiments, except for the number of accumulation = 4096. The  $^{13}\text{C}$  signal intensities obtained by the FSR experiments ( $S_R$ ) were scaled by those obtained by the respective FSR reference experiments ( $S_0$ ), which include no Gaussian  $\pi$  pulse on the  $^{111}\text{Cd}$  channel.

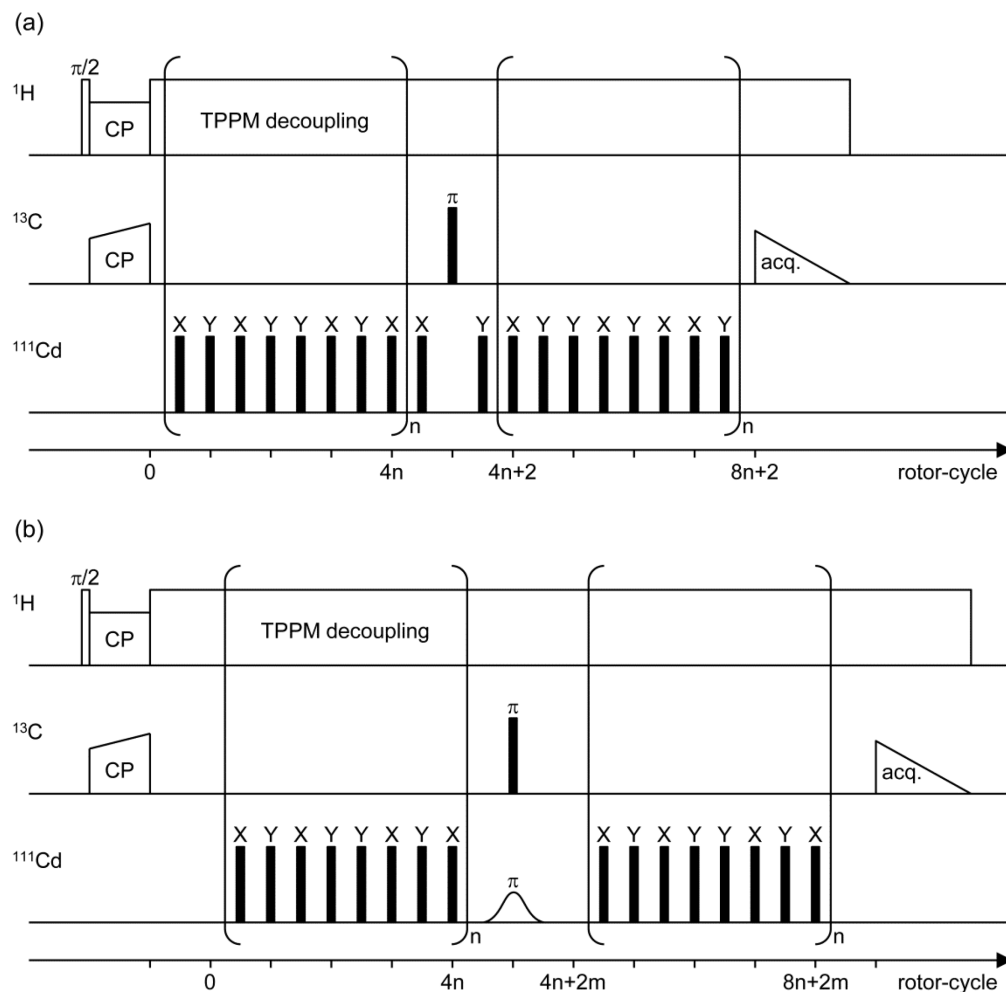


Figure S3. Pulse sequences for (a) REDOR and (b) FSR used in this work. Open rectangles denote  $\pi/2$  pulses, filled rectangles denote  $\pi$  pulses. The rotor-synchronized  $\pi$  pulse train which contains two  $\pi$  pulses per one rotor-cycle is applied to the  $^{111}\text{Cd}$  spins. The number  $n$  means the loop times of the REDOR  $\pi$  pulse train and  $2m$  means the length of a Gaussian  $\pi$  pulse scaled by the rotor-cycle time. In the present FSR experiments, a hard  $\pi$  pulse is irradiated on the  $^{13}\text{C}$  spins and a selective Gaussian  $\pi$  pulse is irradiated on the  $^{111}\text{Cd}$  spins.

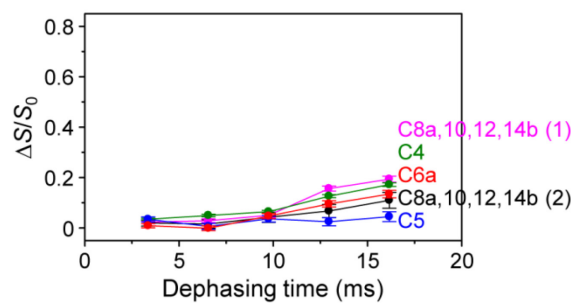


Figure S4. Dephasing time dependence of the  $\Delta S/S_0$  values (the signal intensities of REDOR difference scaled by those of REDOR reference) for the carbons not given in figure 4. The error for each  $\Delta S/S_0$  value was given by

$$\frac{\sqrt{\sigma_0^2 + \sigma_R^2}}{\sigma_0} \cdot \frac{I(S_0)}{I(\Delta S)}$$

where  $\sigma_x$  denotes the standard deviation error of noise in each spectrum and  $I(x)$  denotes the area intensity ( $x = 0$  or  $S_0$  for the REDOR reference spectrum,  $x = R$  for the REDOR spectrum,  $\Delta S$  for the REDOR difference spectrum, respectively). Solid lines are eye guides.

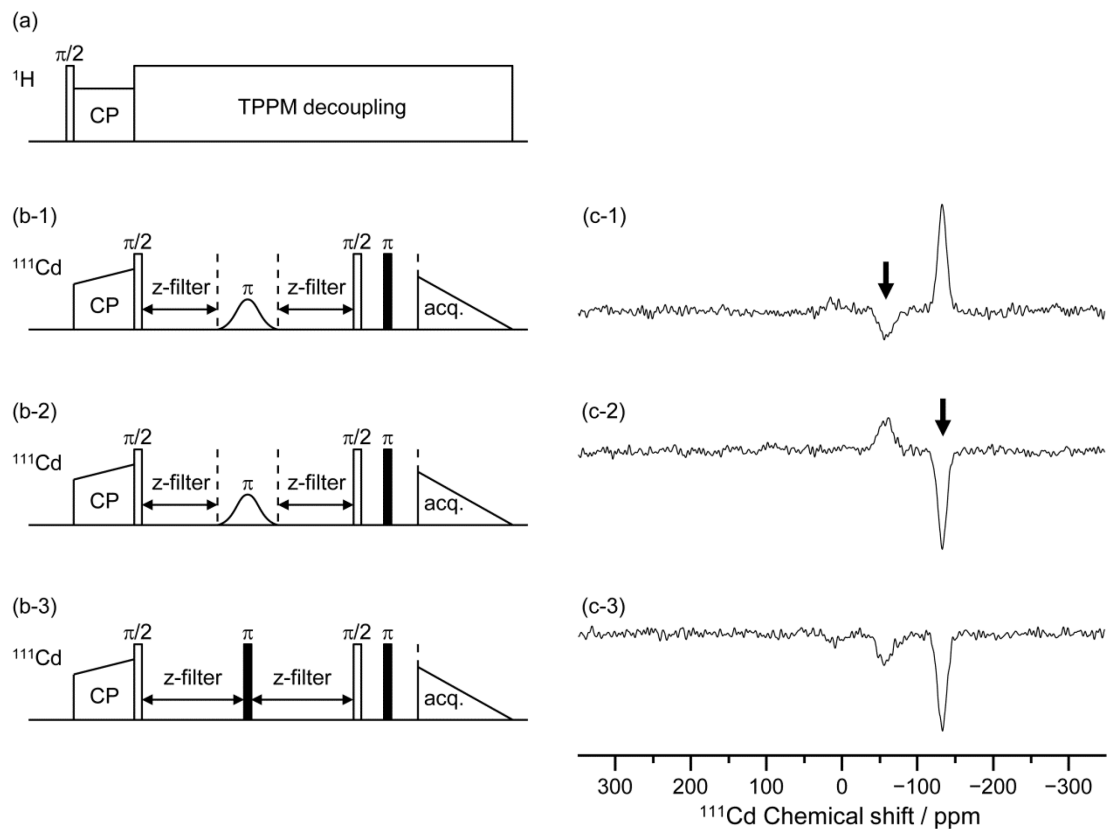


Figure S5. (a, b) Pulse sequences to confirm the selectivity of a  $\pi$  pulse. Schematic pulse sequence diagrams for the  $^1\text{H}$  channel (a) and the  $^{111}\text{Cd}$  channel (b-1, 2, 3) are shown. Figure S3(c-*i*) shows the  $^{111}\text{Cd}$  NMR spectrum obtained by the combination of pulse diagrams (a) and (b-*i*) (*i* = 1, 2 and 3, respectively). A Gaussian  $\pi$  pulse is applied on-resonance to the  $\delta = -50$  ppm (arrow; c-1) or  $\delta = -135$  ppm (arrow; c-2) and a hard  $\pi$  pulse is applied for comparison (b-3). Comparison among (c-1), (c-2) with (c-3) indicates that the Gaussian  $\pi$  pulses slightly lose the magnetization. The intensity of the  $\delta = -50$  ppm signal is reduced to 85%, and that of the  $\delta = -135$  ppm signal is to 97%. The reduction is attributable to the short  $T_2$  of the two  $^{111}\text{Cd}$  signals. This may also affect to reduce the  $\Delta S/S_0$  values of FSR compared to the conventional REDOR.

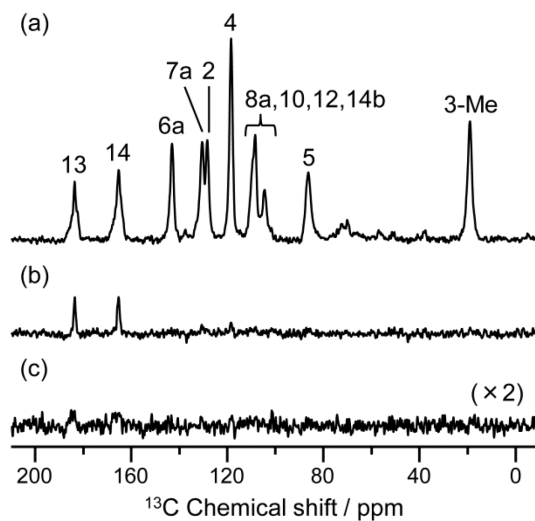


Figure S6. (a)  $^{13}\text{C}$  1D FSR reference ( $S_0$ ) spectrum and (b) difference ( $\Delta S$ ) spectrum of the complex of  $[^{13}\text{C}_{12}]\text{PRM-A}$  at the dephasing time = 9.6 ms. The Gaussian selective  $\pi$  pulse is applied on-resonance to the  $\delta = -135$  ppm signal of  $^{111}\text{Cd}$ . (c)  $^{13}\text{C}$  1D FSR difference ( $\Delta S$ ) spectrum of the complex of  $[^{13}\text{C}_{12}]\text{PRM-A}$  at the dephasing time = 9.6 ms with the Gaussian selective  $\pi$  pulse being applied to the  $\delta = -50$  ppm signal of  $^{111}\text{Cd}$ .

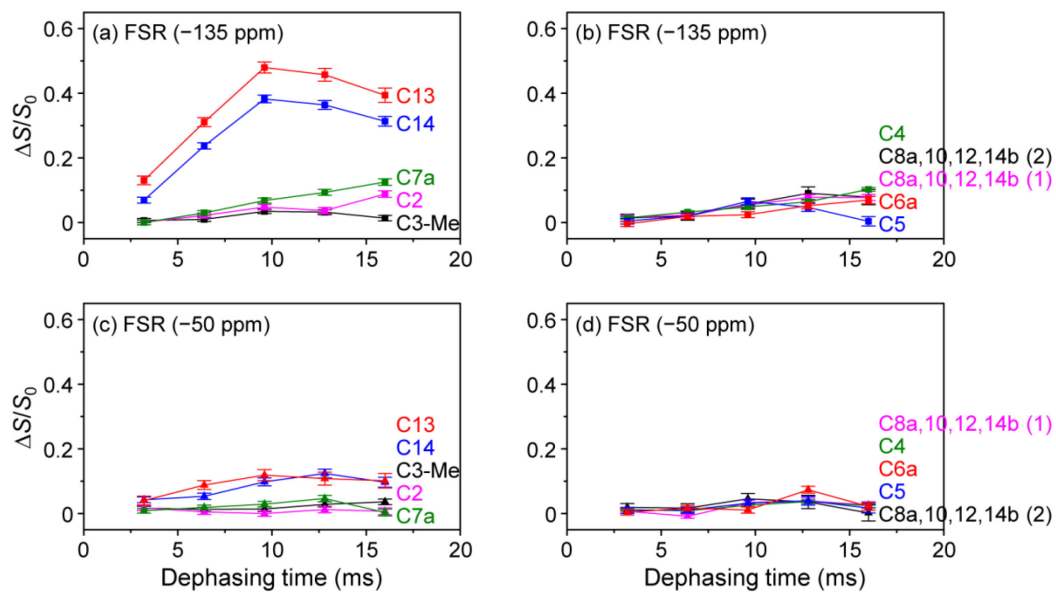


Figure S7. Dephasing time dependence of the  $\Delta S/S_0$  values obtained from the FSR experiment with the Gaussian  $\pi$  pulse applied to (a, b) the  $\delta = -135$  ppm signal of  $^{111}\text{Cd}$  and (c, d) the  $\delta = -50$  ppm signal of  $^{111}\text{Cd}$ . To distinguish clearly, the observed ten  $\Delta S/S_0$  values are collated separately as shown. Error bars were calculated similarly to those given in figure S4. Solid lines are eye guides.

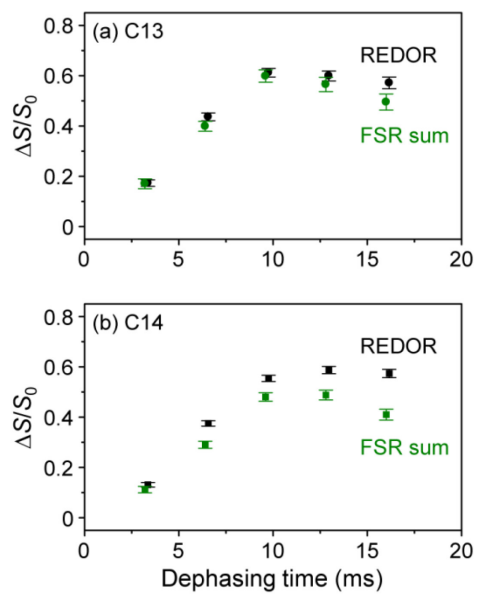


Figure S8. Dephasing time dependence of (a) the C13  $\Delta S/S_0$  values and (b) the C14  $\Delta S/S_0$  values.  $\Delta S/S_0$  values obtained from the REDOR experiment (black), the sum of the  $\Delta S/S_0$  values obtained from the two FSR experiments (green) are plotted. Error bars were calculated similarly to those given in figure S4.



## 9. References for Supporting Information

- [1] Nakagawa, Y., Doi, T., Masuda, Y., Takegoshi, K., Igarashi, Y., and Ito, Y. (2011) Mapping of the primary mannose binding site of pradimicin A. *J. Am. Chem. Soc.* *133*, 17485–17493.
- [2] Gullion, T., and Schaefer, J. (1989) Rotational-echo double-resonance NMR. *J. Magn. Reson.* *81*, 196–200.
- [3] Gullion, T., and Schaefer, J. (1989) Detection of weak heteronuclear dipolar coupling by rotational-echo double-resonance nuclear magnetic resonance. *Adv. Magn. Reson.* vol. 13, W. S. Warren, Ed., Academic Press, New York, 57-83.